HHS Public Access

Author manuscript

Neurotoxicology. Author manuscript; available in PMC 2019 January 01.

Published in final edited form as:

Neurotoxicology. 2018 January ; 64: 204–218. doi:10.1016/j.neuro.2017.05.009.

Manganese exposure induces neuroinflammation by impairing mitochondrial dynamics in astrocytes

Souvarish Sarkar[#], **Emir Malovic**[#], **Dilshan S. Harischandra**, **Hilary A. Ngwa**, **Anamitra Ghosh**, **Colleen Hogan**, **Dharmin Rokad**, **Gary Zenitsky**, **Huajun Jin**, **Vellareddy Anantharam**, **Anumantha G. Kanthasamy**, and **Arthi Kanthasamy**[*]

Parkinson Disorders Research Laboratory, Iowa Center for Advanced Neurotoxicology, Department of Biomedical Sciences, 2062 Veterinary Medicine Building, Iowa State University, Ames, IA 50011

Abstract

Chronic manganese (Mn) exposure induces neurotoxicity, which is characterized by Parkinsonian symptoms resulting from impairment in the extrapyramidal motor system of the basal ganglia. Mitochondrial dysfunction and oxidative stress are considered key pathophysiological features of Mn neurotoxicity. Recent evidence suggests astrocytes as a major target of Mn neurotoxicity since Mn accumulates predominantly in astrocytes. However, the primary mechanisms underlying Mn-induced astroglial dysfunction and its role in metal neurotoxicity are not completely understood. In this study, we examined the interrelationship between mitochondrial dysfunction and astrocytic inflammation in Mn neurotoxicity. We first evaluated whether Mn exposure alters mitochondrial bioenergetics in cultured astrocytes. Metabolic activity assessed by MTS assay revealed an IC_{50} of 92.68 μM Mn at 24 h in primary mouse astrocytes (PMAs) and 50.46 μM in the human astrocytic U373 cell line. Mn treatment reduced mitochondrial mass, indicative of impaired mitochondrial function and biogenesis, which was substantiated by the significant reduction in mRNA of mitofusin-2, a protein that serves as a ubiquitination target for mitophagy. Furthermore, Mn increased mitochondrial circularity indicating augmented mitochondrial fission. Seahorse analysis of bioenergetics status in Mn-treated astrocytes revealed that Mn significantly impaired the basal mitochondrial oxygen consumption rate as well as the ATP-linked respiration rate. The effect of Mn on mitochondrial energy deficits was further supported by a reduction in ATP production. Mn-exposed primary astrocytes also exhibited a severely quiescent energy phenotype, which was substantiated by the inability of oligomycin to increase the extracellular acidification rate. Since astrocytes regulate immune functions in the CNS, we also evaluated whether Mn modulates astrocytic inflammation. Mn exposure in astrocytes not only stimulated the release of

[*]To whom correspondence should be addressed: Arthi Kanthasamy, Ph.D. Professor, Department of Biomedical Sciences, Iowa State University, Ames, IA 50011, Telephone: (515) 294-2516; Fax: (515) 294-2315, arthik@iastate.edu.
[#]These authors made equal contributions

Conflict of interest: A. G.K. and V.A. are shareholders of PK Biosciences Corporation (Ames, IA), which is interested in identifying novel biomarkers and potential therapeutic targets for PD. A.G.K and V.A Do not have any direct interest in the work presented in present work.

proinflammatory cytokines, but also exacerbated the inflammatory response induced by aggregated α-synuclein. The novel mitochondria-targeted antioxidant, mito-apocynin, significantly attenuated Mn-induced inflammatory gene expression, further supporting the role of mitochondria dysfunction and oxidative stress in mediating astrogliosis. Lastly, intranasal delivery of Mn *in vivo* elevated GFAP and depressed TH levels in the olfactory bulbs, clearly supporting the involvement of astrocytes in Mn-induced dopaminergic neurotoxicity. Collectively, our study demonstrates that Mn drives proinflammatory events in astrocytes by impairing mitochondrial bioenergetics.

Introduction

Central nervous system (CNS) aberrations resulting from prolonged exposure to transition metals such as iron (Febbraro et al., 2012; Galvin et al., 2000; Gregory et al., 2009), lead (Bihaqi and Zawia, 2013), and manganese (Gorojod et al., 2015; Hesketh et al., 2008), lend support to the potential involvement of environmental metal exposure in etiology of chronic neurodegeneration (Rokad et al., 2016). Manganese (Mn) toxicity resulting from overexposure to airborne sources was first noted in miners (Peres et al., 2016; Rodier, 1955), and subsequently in industrial workers like welders (Horning et al., 2015; Kwakye et al., 2015). Although Mn has a multitude of physiological functions (e.g., enzyme cofactor for superoxide dismutase and arginase, immunity, bone development, and reproduction) (Karki et al., 2015), the accruing toxic levels has been shown to predominately localize to the globus pallidus, as well as other brain areas of the extrapyramidal motor system, thereby leading to a condition termed manganism, which is phenotypically similar to PD (Kwakye et al., 2015; Milatovic, D. et al., 2007). In addition, diets including grains, legumes, baby formulations and nuts represent the main source of Mn, of which <5% is intestinally absorbed (Karki et al., 2013; Kwakye et al., 2015). Approximately, 30-40% of inhaled Mn is absorbed into the bloodstream, where it is transported primarily bound to albumin and β-globulin in oxidation state 2 (Mn^{2+}) (Karki et al., 2013); however, the absorbed proportion could be smaller (~10.6%) because of oxidative state-dependent differences in solubility (Ellingsen et al., 2003). Availability of the Mn^{2+} oxidation state in the central nervous system (CNS) is facilitated by transporters such as divalent metal ion transporter 1 (DMT1) and SLC13A10, while Mn^{3+} is facilitated by transferrin (Chen et al., 2015; Karki et al., 2015; Leyva-Illades et al., 2014; Sidoryk-Wegrzynowicz and Aschner, 2013).

As a ubiquitous constituent and physiological glue of the CNS, astrocytes are indispensable for cellular homeostatic maintenance (Volterra and Meldolesi, 2005). Astrocytes regulate extracellular glutamate levels among neurons in tripartite synapses (Karki et al., 2013; Popoli et al., 2011). Excessive Mn can disrupt this regulation by inducing tumor necrosis factor-α (TNFα), a secreted proinflammatory cytokine. Previous studies demonstrated that Mn impairs calcium (Ca^{2+}) homeostasis in astrocytes and activates key proinflammatory events such as NFκB, *NOS2* and cytokine production (Karki et al., 2015; Karki et al., 2014). This inflammatory response increases expression of yin yang-1, a transcription repressor that inhibits production of excitatory amino acid transporter-2, which is necessary for glutamate reuptake (Karki et al., 2015; Karki et al., 2014). Recent studies also demonstrate that Mn interferes with neurodegenerative disease-specific proteins including prions, alpha-synuclein

and huntingtin (Bichell et al., 2017; Choi et al., 2010; Choi et al., 2007; Harischandra et al., 2015), as well as protein misfolding, which may further contribute to neuroinflammation. Thus, Mn exposure can activate the inflammatory response in astrocytes, which can further contribute to Mn neurotoxicity.

Along with pericytes, the end-feet of astrocytes envelope blood vessels to regulate blood-brain barrier trafficking (Pekny and Pekna, 2014). Interestingly, astrocytes have been demonstrated to have an increased affinity for Mn, with concentrations up to 50-fold greater than in neurons (Aschner et al., 1992; Gonzalez et al., 2008). Once internalized, the Mn is sequestered by mitochondria via the Ca^{2+} uniporter (Gunter et al., 2006). Kinetical analyses revealed the influx of Mn through this mitochondrial uniporter is slower than Ca^{2+} *per se*, but Mn efflux is far slower (Gavin et al., 1990; Martinez-Finley et al., 2013). Even though the atomic charge properties and size of Mn are quite analogous to Ca^{2+}, the two Ca^{2+} efflux mechanisms are poor exporters of Mn, thus explaining the mitochondrial sequestration of Mn (Gunter et al., 1975; Gunter and Sheu, 2009; Martinez-Finley et al., 2013). On the other hand, although sodium (Na^{+})-independent Ca^{2+} efflux does transport Mn, Na^{+}-dependent Ca^{2+} efflux, the predominant mechanism in CNS mitochondria, has not been reported to export Mn (Gavin et al., 1990; Gunter and Sheu, 2009; Martinez-Finley et al., 2013). This extremely sluggish efflux of Mn potentially explains the prolonged CNS clearance and the buildup of toxicity (Martinez-Finley et al., 2013). Mn can also competitively inhibit both efflux pathways, thereby raising the mitochondrial Ca^{2+} concentration, which can impair aerobic respiration and elicit reactive oxygen species (ROS) generation (Gavin et al., 1990; Martinez-Finley et al., 2013; Streifel et al., 2013; Tjalkens et al., 2006).

Despite the known effects of Mn on astrocytes, the extent of Mn-induced structural and functional impairment of mitochondrial dynamics and its consequent neuroinflammatory processes as it relates to Mn neurotoxicity have not been systematically examined. In the present study, we characterized the impact of Mn on mitochondrial bioenergetic flux in astrocytes using the Seahorse bioenergetic analyzer and its functional consequence on neuroinflammation. Our results demonstrate that overexposure to Mn i) lowers basal respiration in astrocytes, ii) induces astrocytic inflammation that is not exclusive to TNFα, and iii) potentiates aggregated α-Synuclein (αSyn_{agg})-induced inflammation in astrocytes. Thus, our study establishes a functional interaction between mitochondrial dysfunction and astrocytic inflammation in Mn-induced neurotoxicity. In addition, we report that the mitochondria-targeted anti-oxidant mito-apocynin attenuates Mn-induced astrocyte inflammation.

Methods

Chemicals and Reagents

Dulbecco's modified eagle medium (DMEM), fetal bovine serum (FBS), L-glutamine (Q), and penicillin/streptomycin (P/S) were obtained from Invitrogen (Carlsbad, CA). MitoTracker Green FM and MitoTracker Red CMXRos, were purchased from Molecular Probes (Eugene, OR). Manganese Chloride ($MnCl_2$) was obtained from Sigma-Aldrich (St. Louis, MO). The CellTiter® 961 AQueous Non-Radioactive Cell Proliferation Assay kit and CellTiter® Glo Luminescent Cell Viability Assay kit were obtained from Promega

(Madison, WI). The CD11b magnetic separation kit was purchased from Stem Cell Technologies (Vancouver, Canada). Tyrosine hydroxylase (TH) (AB_2201528) and glial fibrillary acidic protein (GFAP) (AB_2109815) antibodies were purchased from EMD Millipore. Inducible nitric oxide synthase (iNOS) (AB_631831) antibody was purchased from Santa Cruz Biotechnologies (Dallas, TX). Mitofusin-2 (Mfn2) (#11925) was purchased from Cell Signaling Technologies. All the standards used for the Luminex multiplex cytokine assay were purchased from PeproTech Inc (Rocky Hill, NJ). Streptavidin-Biotin and biotinylated antibodies used for Luminex were purchased from eBioSciences (San Diego, CA). MA was obtained from Dr. Kalyanaraman (Medical College of Wisconsin, Milwaukee).

Animal Study

Eight-week-old male C57BL/6Ncrl mice, obtained from Charles River, were housed under standard conditions of constant temperature (22 ± 1°C), humidity (relative, 30%), and a 12 h light/dark cycle. After acclimating for 3 days, mice were exposed to 50 μL of 20 mM of Mn (200 μg). This dose is consistent with previously published literature (Moberly et al., 2012). According to reports from Centers for Disease Control and Prevention, the ambient level of Mn near industries is 0.2-0.33 mg/m^3. Hence the dose used is environmentally relevant (https://www.atsdr.cdc.gov/toxprofiles/tp151-c2.pdf). Use of the animals and protocol procedures were approved by the Institutional Animal Care and Use Committee (IACUC) at Iowa State University (Ames, IA, USA). Intranasal delivery was preferred because it takes advantage of an incomplete blood-brain barrier in the olfactory epithelium. The olfactory nerves can completely bypass the blood-brain barrier, thus chemicals can be taken up by these neurons and transported directly into the brain (Graff and Pollack, 2005). Also, environmental exposure is usually occupation-related inhalation. Following the treatments, we carried out behavioral, biochemical and neurochemical studies.

Cell culture and Treatments

One-day-old C57BL/6Ncrl pups were sacrificed, their brains dissected out, and a single cell suspension was prepared. After growing in culture for 16 days, the astrocytes were isolated after microglia were removed using our CD11b magnetic-bead separation technique (Gordon et al., 2011; Sarkar et al., 2017). The human astrocytic U373 cell line was obtained from ATCC and grown per ATCC protocol. Primary mouse astrocytes (PMAs) were cultured in DMEM, 10% FBS, 1% Q, 1% P/S. Treatments for PMAs were performed in 2% FBS-containing DMEM, with 1% Q and P/S. U373s were cultured in MEM, 10% FBS, 1% Q, and 1% P/S. Treatments for U373s were performed in 2%-FBS-containing MEM, with 1% Q and P/S. All treatments were for 24 h using Mn at 100 μM, αSyn_{agg} at 1 μM, and mito-apocynin at 10 μM.

Recombinant human α-synuclein purification and aggregation

BL21(DE3) strain *E. coli* cells were transformed using a plasmid encoding for wild-type human α-synuclein and grown on agar plate with Ampicillin (Amp) resistance. Pre-culture was prepared by inoculating a single colony from the agar plate into a tube containing 10 mL of LB broth with Amp and incubated overnight at 37 °C. The following day, the pre-culture was inoculated into 1 L of LB medium containing Amp, and OD_{600} was taken every

hour till the culture reached an OD of 0.5. Recombinant α-synuclein expression was induced by adding 1 mM isopropyl β-D-1-thiogalactopyranoside (IPTG) (Invitrogen), and the cells were further incubated at 37 °C for 8 h before harvesting. Cells were lysed and recombinant α-synuclein was purified as previously described (Giasson et al., 1999; Narhi et al., 1999). Finally, protein was lyophilized and stored at -80 °C. For α-synuclein aggregation, a 70-μM recombinant protein solution was prepared by dissolving 1 mg in 1 mL of ultrapure water and shaken at a speed of 1000 rpm at 37 °C for 7 days (Luk et al., 2012b).

qRT-PCR

RNA extraction and qRT-PCR were performed as described previously(Gordon, R. et al., 2016a; Seo et al., 2014). Total RNA was extracted using TRIZOL reagent as per the manufacturers' protocol and concentration was measured using NanoDrop. First strand cDNA synthesis was performed using an Affinity Script qPCR cDNA synthesis system (Agilent Technologies). Real-time PCR was performed with the RT2 SYBR Green master mix (Thermo-Fisher #K0172). The following genes from QuantiTect Primer Assay (Qiagen) were used for qRT-PCR: pro-IL-1β, pro-IL-18, CSF-2, IL-12b, and IL-6. The house keeping gene 18S rRNA (Qiagen #PPM57735E) was used as the reference for all qRT-PCR experiments. The dissociation curves were run to ensure a single amplicon peak was obtained. The results are reported as fold change in gene expression, which was determined via the ΔΔCt method using the threshold cycle (Ct) value for the housekeeping gene and for the respective gene of interest in each sample (Gordon, Richard et al., 2016; Lawana et al., 2017).

Western Blotting

Western blot analysis was performed according to previous published protocols (Harischandra et al., 2017; Kanthasamy et al., 2012). Briefly, tissue/cell samples were homogenized using a tissue homogenizer in RIPA buffer. Following protein isolation, the Bradford assay was performed for protein estimation. Next, 25-40 μg of protein was loaded in each well of 10-15% SDS-acrylamide gels and ran for 2 h at 110 V. After running, proteins were transferred to a nitrocellulose membrane at 27 V for 18 h at 4°C. After transfer, the membranes were blocked using LI-COR blocking buffer for 1 h at RT. Following blocking, the membranes were incubated in primary antibodies for 3 to 18 h, then washed with PBS-Tween (0.01%), incubated in infrared LI-COR secondary antibodies for 1 h, then washed again with PBS-Tween, and scanned using LI-COR scanner. The following antibodies were used: GFAP (1:1000), TH (1:1000), and iNOS (1:500). Secondary antibodies were used according to manufacturer's instructions.

Luminex Multiplex Cytokine Analysis

Cytokine levels were assessed via Luminex cytokine assay according to our previous publications (Gordon, R. et al., 2016b; Panicker et al., 2015). Briefly, PMAs were treated in 96-well plates (20,000 cells/well) with 100 μL of treatment medium. Post-treatment, 40 μL of the treatment medium was collected and added to 40 μL of primary antibody conjugated to magnetic microspheres and incubated overnight at 4°C in a clear bottom, black 96-well plate. For serum cytokine levels, serum was diluted 5 times with block/store buffer containing BSA (Sigma-Aldrich), and 40 μL of diluted serum was used as the sample. After

incubation, each well was triple-washed using a magnetic washer and then incubated for 1 h with secondary antibodies followed by three more washes. Lastly, samples were incubated for 30 min with streptavidin/phycoerythrin followed by another two washes. A Bio-Plex reader was used to read the 96-well plates.

MTS Assays

MTS assay was performed according to our previous publications (Brenza et al., 2016; Charli et al., 2016). Briefly, 20,000 cells/well were plated in a 96-well tissue culture plate and exposed to 100 μL of treatment medium after attachment. Post-treatment, 10 μL of MTS dye was added to each well and incubated for 45 min at 37°C. After incubation, absorbance readings were taken using a plate reader at 490 nm, and a 640-nm readout was used for background subtraction.

Seahorse Mito-Stress Analysis

A Seahorse XFe24 Analyzer was used to measure mitochondrial extracellular acidification rates (ECAR) and oxygen consumption rates (OCR) using the Mito-Stress test following a previously published protocol (Charli et al., 2016). PMAs were plated at 20,000 cells/well of a Seahorse plate. The calibration plate was hydrated overnight in a non-CO_2 incubator. For the Mito-Stress test, 0.75 μM oligomycin, 1 μM FCCP, and 0.5 μM rotenone/antimycin were used. The wave report generator (Agilent) and cell-phenotype report generator were used for analysis.

MitoTracker Green FM and MitoTracker Red CMXRos

MitoTracker Green FM and MitoTracker Red CMXRos were obtained from Molecular Probes and used according to our previous publications (Charli et al., 2016; Gordon, Richard et al., 2016). After treatment, cells were washed and incubated in MitoTracker green FM according to the concentration suggested by the manufacturer for 10-20 min in HBSS, followed by washing with HBSS. Hoechst nuclear stain was used to normalize the results. Excitation and emission readings were taken using a plate reader with 490 and 516 nm, respectfully, for MitoTracker green FM and 350 and 461 nm for Hoechst. For the MitoTracker Red CMXRos assay, post-treatment cells were washed in fresh media and incubated in MitoTracker red dye (200 nM) for 15 min. Following incubation, cells were washed twice, fixed in 4% paraformaldehyde, mounted on slides, dried overnight, and imaged using a Nikon Eclipse C1 microscope equipped with a SPOT RT3 digital camera (Diagnostic Instruments, Sterling Heights, MI).

ATP Assay

ATP assay was performed following Charli *et al.* (2016) with minor modifications. Briefly, 20,000 cells/well were plated in an opaque 96-well plate and exposed to 100 μL of treatment medium after attachment. After treatment, 100 μL of CellTiter-Glo Luminescent reagent from Promega was added to each well containing 100 μL of media. The samples were placed on an orbital shaker for 3 min after which they were incubated for 10 min at RT. Readings were taken using a luminometer (BioTek). Background luminescence was determined using

the corresponding cell-free treatment media and the average was subtracted from the sample values.

HPLC analysis

HPLC analysis of dopamine was performed according to our previous publication (Gordon, Richard et al., 2016). In brief, olfactory bulb tissues were extracted using an antioxidant extraction solution (0.1 M perchloric acid containing 0.05% Na_2EDTA and 0.1% $Na_2S_2O_5$) and isoproterenol (internal standard). A reversed-phase C-18 column was used to isocratically separate dopamine, 3,4-dihydroxyphenylacetic acid (DOPAC), and homovanillic acid (HVA) at a flow rate of 0.6ml/min using a Dionex Ultimate 3000 HPLC system (pump ISO-3100SD, Thermo Scientific, Bannockburn, IL) equipped with a refrigerated automatic sampler (model WPS-3000TSL). The electrochemical detection system included a CoulArray model 5600A coupled with an analytical cell (microdialysis cell 5014B) and a guard cell (model 5020) with potentials set at 350, 0, -150, and 220 mV. Data acquisition and analysis were performed using Chromeleon 7 and ESA CoulArray 3.10 HPLC Software.

Behavior Analysis

The automated VersaMax Monitor (model RXYZCM-16, AccuScan, Columbus, OH) was used to measure the spontaneous open-field locomotor activity of mice in an activity chamber made of clear Plexiglas and covered with a ventilated Plexiglas lid, as described previously (Ghosh et al., 2013; Ngwa et al., 2014). Horizontal and vertical activity data were collected and analyzed by a VersaMax Analyzer (model CDA-8, AccuScan). Locomotor activities were monitored during a 10-min test session following a 2-min acclimation period.

Data Analysis

GraphPad 5.0 was used for statistical analysis with $p \leq 0.05$ considered statistically significant. One-way ANOVA was used for comparison among multiple groups. In most cases, Tukey post analysis was applied. For comparing 2 groups, Student's t-test was used.

Results

Mn induced a dose-dependent decrease in mitochondrial metabolic activity in astrocytes

Mn has been shown to accumulate in mitochondria, block the electron transport chain (ETC), and alter mitochondrial permeability in astrocytes (Hazell, 2002; Rao and Norenberg, 2004). In this experiment, we examined the effect of Mn on metabolic activity in PMA and U373 cells. Both sets of astrocytes were exposed to increasing concentrations of Mn (0.001-1 mM) for 24 h. We observed a dose-dependent decrease in metabolic activity as determined by MTS assay. The IC_{50} for inhibiting metabolic activity was determined to be 92.7 μM for PMAs (Fig. 1A) and 50.5 μM for U373s (Fig.1B). Thus, we used 100 μM Mn for all subsequent studies. To further validate the effect of Mn on astrocytic mitochondria, both PMAs and U373s were treated with 100 μM Mn for 24 h, and then subjected to MitoTracker green, a fluorescent dye that binds to intact mitochondria in live cells irrespective of mitochondrial potential and its intensity indicates mitochondrial health. In this assay, we observed a statistically significant loss of mitochondrial mass, suggesting a

loss of mitochondrial function in PMAs (Fig. 2A) and U373s (Fig. 2B) compared to untreated controls. Additionally, we used MitoTracker red dye to verify mitochondrial morphology in Mn treated PMAs (Fig. 2C). Mn exposure was found to increase mitochondrial circularity, indicating augmentation of mitochondrial fission (Scott and Youle, 2010), and it positively correlated with diminished ATP production in PMAs as determined by CellTiter-Glo Luminescent assay (Fig. 2D). Furthermore, qRT-PCR analysis revealed that transcript levels of *Mfn2*, a gene involved in mitochondrial fusion and linked to PD pathology (Tang et al., 2015), was down-regulated in response to Mn treatment (Fig. 2E). Immunoblot analysis further showed that Mn exposure downregulated Mfn2 protein levels (Fig. 2F). Together, these data suggest that Mn treatment reduces metabolic activity, mitochondrial mass, and dysregulates mitochondrial fission/fusion processes in both mouse and human astrocytes.

Altered mitochondrial dynamics and bioenergetics in Mn-treated astrocytes

Mn is known to alter brain mitochondrial influx/efflux kinetics, which affects energy metabolism (Gavin et al., 1990). Thus, we examined the effects Mn treatment exerts on mitochondrial bioenergetics using the Seahorse XFe24 analyzer as described in our recent publication (Charli et al., 2016). PMAs were treated with 100 μM Mn for 24 h, after which the Mito Stress assay was performed (Fig. 3 and 4). The Seahorse directly measures oxygen consumption rate (OCR) (Fig. 3A), while also monitoring the extracellular acidification rate (ECAR), an indicator of glycolysis (Fig. 4A). Mn exposure led to a statistically significant decrease in basal mitochondrial respiration and in oxygen consumption (Fig. 3A-B) when compared to untreated PMAs. Similarly, Mn exposure also reduced mitochondrial ATP production (Fig. 3A,C) as well as the non-mitochondrial respiration rate (Fig. 4A-B). Thus, Mn not only diminishes astrocytic mitochondrial function, but also markedly reduces glycolytic function. Additionally, cell phenotype analysis revealed that Mn exposure shifts the astrocytes' bioenergetic phenotype from aerobic to a quiescent state (Fig. 4C). These data collectively suggest that Mn exposure not only lowers the basal respiration rate and ATP production, but also alters the cellular phenotype by lowering glycolytic flux.

Upregulation of inflammatory genes in Mn-treated astrocytes

Although the role of mitochondrial bioenergetics has been well established in PD models, most of that research focused on neurons. More recent studies have suggested a potential link between neuroinflammation and mitochondrial defects in neuroimmune cells that may contribute to the amplification of inflammatory and neurodegenerative processes (Alfonso-Loeches et al., 2014). To test for a potential link between mitochondrial dysfunction and inflammation in astrocytes, we treated PMAs with 100 μM Mn for 24 h. The cells were then subjected to qRT-PCR analyses and the treatment media were analyzed for the release of pro-inflammatory cytokines. As revealed by qRT-PCR, Mn treatment increased mRNA levels of the pro-inflammatory factors *IL-12b* (Fig. 5A), *IL-6* (Fig. 5B), *TNFα* (Fig. 5C), *NOS2* (Fig. 5D), *pro-IL-1β* (Fig. 5E) and CSF-2 (Fig. 5F). Luminex cytokine assay revealed that Mn induced the release of the pro-inflammatory cytokines IL-6 (Fig. 5G), IL-12 (Fig. 5H), and TNFα (Fig. 5I) in the extracellular milieu. These data suggest that Mn can activate astrocytes, leading to the induction and maturation of pro-inflammatory factors.

Mn potentiates αSyn$_{agg}$-induced inflammation in astrocytes

Misfolded αsyn (*PARK1,4*) has been linked to PD pathogenesis and is one of the major components of Lewy bodies (Kim et al., 2013). In terms of gene-environment interaction between αsyn and Mn, our study showed that prolonged exposure to Mn induces αsyn aggregation (Harischandra et al., 2015). Furthermore, we and others have shown that αSyn$_{agg}$ induces inflammation in microglia and astrocytes (Codolo et al., 2013; Gordon, R. et al., 2016b; Kim et al., 2013; Su et al., 2008). Hence, we hypothesized that exposure to an environmental toxicant like Mn in tandem with αSyn$_{agg}$ will either have an additive or synergistic effect on inflammation. PMAs were treated with either 100 μM Mn plus 1 μM αSyn$_{agg}$, 100 μM Mn alone or 1 μM αSyn$_{agg}$ for 24 h, and then the cells were harvested and treatment media were subjected to qRT-PCR and Luminex assays. As revealed by qRT-PCR analysis, Mn synergistically increased the αSyn$_{agg}$-induced expression of *pro-IL-1β* (Fig. 6A) and the release of IL-1β (Fig. 6B). Mn had an additive effect on the αSyn$_{agg}$-induced pro-inflammatory factor *IL-6* (Fig. 6C) and it potentiated the αSyn$_{agg}$-induced increase in *CSF-2* (Fig. 6E). Furthermore, Mn potentiated the αSyn$_{agg}$-induced release of the pro-inflammatory cytokines IL-12 (Fig. 6D) and TNFα (Fig. 6F). Collectively, these data indicate that Mn exposure exacerbates inflammation elicited by αSyn$_{agg}$ in astrocytes.

Mito-apocynin, a novel mitochondrially targeted derivative of apocynin, attenuated Mn-induced inflammatory genes in human astrocytic culture

Our group has recently shown that mito-apocynin, a novel mitochondrially targeted derivative of apocynin, can reduce inflammation and neurodegeneration in an MPTP mouse model of PD by reducing mitochondria-mediated oxidative stress (Ghosh et al., 2016a). If Mn-induced mitochondrial ROS contributes to astrocytic neuroinflammatory processes, then the anti-oxidant mito-apocynin should dampen Mn-induced inflammation in human astrocytic culture. U373s were co-treated with 100 μM Mn and 10 μM mito-apocynin for 24 h. Following treatment, cells were collected for mRNA analysis. As revealed by qRT-PCR, mito-apocynin significantly reduced the expression level of the pro-inflammatory factors, *pro-IL-1β* (Fig. 7B), and *pro-IL-18* (Fig. 7C) induced by Mn alone. Mito-apocynin further reduced the expression of *CSF*-2 (Fig. 7A). Lastly, the MitoTracker green assay revealed that mito-apocynin prevented the Mn-induced reduction of astrocytic mitochondrial mass (Fig. 7D). These data collectively suggest that the mitochondrially targeted anti-oxidant mito-apocynin protects against Mn-induced inflammation in astrocytes by possibly dampening mitochondrial oxidative stress.

Intranasal delivery of Mn induces inflammation and TH loss in the olfactory bulbs of mice

To validate our findings from primary astrocyte cultures in animal models, we subjected C57BL/6 mice to intranasal doses of 200 μg Mn in 50 μL three times a week for four weeks. At the end of the treatment period, behavioral tests were performed and then OB tissues were collected for neurochemical and biochemical analyses. Mn reduced motor activity, as indicated by the significant reduction in total distance traveled (Fig. 8A), horizontal activity (Fig. 8B), and total movement time (Fig. 8C). Furthermore, neurochemical analysis of the olfactory bulb revealed that intranasal delivery of Mn significantly decreased dopamine levels (Fig. 8D), which coincided with a downregulation of TH expression (Fig. 8E).

Immunoblot analysis of OB tissues showed that Mn induced the expression of GFAP, an activation marker of astrocytes (Fig. 8F). Additionally, iNOS expression (Fig. 8G) and serum IL-12 (Fig. 8H) were elevated, indicating that Mn elicited a pro-inflammatory response. Although Mn has been shown to accumulate in the striatal region, we did not observe any changes in striatal pro-inflammatory factors or TH levels (data not shown) even after 30 days. Together these data corroborate our *in vitro* findings, whereby Mn-induced astroglial activation is accompanied by an enhanced pro-inflammatory response.

Discussion

Neuroinflammation plays a key role in neurodegenerative disorders, including Parkinsonian syndrome (Glass et al., 2010; Golde, 2002; Herrero et al., 2015; Tansey and Goldberg, 2010; Whitton, 2007). Even though the etiology of these diseases is not well established, the consensus is that environment plays an important role in these neurodegenerative disorders. Astrocytes, the most abundant glial cells of the brain, are a recognized source of sustained inflammation upon activation (Phillips et al., 2014). Besides showing how the environmental neurotoxin Mn affects astrocytes, we also demonstrate its role in triggering a synergistic interaction between mitochondrial dysfunction and inflammation. Here, we show that Mn inhibits astrocytic metabolic activity and further contributes to mitochondrial dysfunction at a lower micromolar concentration than reported elsewhere for a 24-h IC_{50} (Gonzalez et al., 2008; Park and Park, 2010; Yin et al., 2008). For the first time, we demonstrate via the Seahorse bioanalyzer that Mn exposure can change the metabolic phenotype of astrocytes. We also show that Mn exposure increased the release of pro-inflammatory factors from astrocytes and potentiated the release of IL-1β initially induced by αSyn_{agg}. Finally, we demonstrate *in vivo* that intranasal Mn exposure increased astrocytic activation, motor deficits and the loss of TH.

Although several studies have suggested that Mn induces mitochondrial dysfunction and impairs glutamate uptake in astrocytes (Milatovic, D. et al., 2007; Rao and Norenberg, 2004), none have linked mitochondrial dysfunction to inflammation. The accumulation of Mn in mitochondria induces mitochondrial dysfunction by increasing oxidative stress and impairing membrane potential (Hazell, 2002; Milatovic, Dejan et al., 2007; Rao and Norenberg, 2004). Our findings further support the role of Mn toxicity in astrocytic and mitochondrial dysfunction. We show Mn-induced mitochondrial dysfunction is associated with decreased mitochondrial mass and reduced expression of the mitochondrial fusion protein Mfn2 (Fig. 2). Mfn2 reduction has been linked to progressive loss of dopaminergic neurons in the nigrostriatal tract (Pham et al., 2012). Furthermore, recent studies have shown that VPS35 (PARK17) modulates Mfn2 degradation leading to mitochondrial dysfunction in dopaminergic neurons (Tang et al., 2015). On the other hand, Mfn2 overexpression can reduce astrogliosis *in vitro* (Liu et al., 2014). From the bioenergetic profile, we found that basal oxygen consumption and maximal respiratory capacity were significantly attenuated by Mn, indicating that Mn damages mitochondrial function, as further evidenced by a parallel reduction in ATP levels. Interestingly ECAR, which serves as an index of glycolysis, was reduced in cells exposed to Mn as compared to control cells. A previous study involving U87 astrocytoma cells reported a concentration-dependent decrease in the activity of several glycolytic enzymes such as hexokinase, lactate dehydrogenase, and pyruvate kinase

(Malthankar et al., 2004). Based on this study, the inhibition we observed may not be a direct effect of Mn, but rather a secondary impairment following the disruption of the electron transport chain and tricarboxylic acid cycle. Our studies raise the possibility that Mn can also inhibit glycolysis, thereby accounting for the pronounced depletion of ATP in Mn-treated cells (Fig. 2), but further studies will be essential to understand the role glycolytic flux under different Mn exposure times. Astrocytes provide neurotrophic and nutrient support to neighboring neurons by producing growth factors and helping to maintain neuronal function, tissue repair, and homeostasis. In contrast, reactive astroglia produce proinflammatory factors, which become toxic to neurons when persistently activated under chronic stress, thus leading to degeneration. The phenotypic switch observed in our study upon exposure to Mn may limit nutrient availability, thereby contributing to neuronal stress.

Although microglia are the major inflammatory cells in the brain, recent studies have identified astrocytes to also be a key player driving neuroinflammation and neurodegeneration (Colombo and Farina, 2016). A few studies have suggested a possible link between Mn and inflammation in astrocytes (Hazell, 2002; Moreno et al., 2009; Moreno et al., 2008), however, the signaling mechanisms associated with this inflammation remain elusive. In this study, we demonstrate that exposing astrocytes to Mn induced the expression and release of pro-inflammatory factors such as IL-1β, TNFα and IL-6 (Fig. 5). Recently, IL-1β has been linked to inflammasome signaling, which has been implicated in various neurodegenerative disorders (Freeman and Ting, 2016). In particular, the multi-protein NLRC4 inflammasome complex has been implicated in the inflammatory signaling process in astrocytes (Liu and Chan, 2014). We are currently investigating the role of these inflammasomes in the Mn-induced inflammatory cascade in astrocytes.

Aggregated α-synuclein is the key constituent of Lewy bodies, and has been shown to be secreted from stressed or dying neurons. Microglia cells can be activated by secreted αSyn_{agg}, thereby inducing inflammation in PD (Alvarez-Erviti et al., 2011; Kim et al., 2013; Lee et al., 2010; Lotharius and Brundin, 2002; Luk et al., 2012a; Su et al., 2008). Our group has previously demonstrated that long-term Mn exposure induces αSyn aggregation leading to neuronal death (Harischandra et al., 2015). We recently demonstrated that other divalent metals like copper interact with prion proteins to promote aggregation (Yen et al., 2016). In this study, we demonstrate for the first time that Mn can also potentiate an αSyn_{agg}-induced inflammatory response in astrocytes, further fueling the possibility of a gene-environment interaction driving inflammation and neurodegeneration (Fig. 6).

The role of ROS generation in inflammation and neurodegenerative disorders has been well documented (Amor et al., 2010; Mittal et al., 2014). Furthermore, oxidative stress has been linked to Mn-induced neurotoxicity (Chen and Liao, 2002). In fact, in a recent report using antioxidants, resistance was conferred against neurotoxicity (Ghosh et al., 2016b) by reducing inflammation and oxidative stress in a neurotoxin model of PD. We also recently demonstrated that mito-apocynin, a mitochondrially targeted derivative of apocynin, can reduce inflammation in the MPTP mouse model of PD (Ghosh et al., 2016a). We have since demonstrated that mito-apocynin reduces mitochondrial superoxide generation in neuronal cells as well as oxidative damage in MitoPark mice, a mitochondrially defective animal model of PD (Langley et al., 2017). In this study, we demonstrate that mito-apocynin

attenuated the Mn-induced inflammatory response in astrocytes by mitigating Mn's effect on mitochondrial mass (Fig. 7). This further confirms that mitochondrial damage can directly augment inflammation in astroglial cells.

Intranasal delivery of Mn can cause deficits in both spatial memory and motor function (Blecharz-Klin et al., 2012). Likewise, in our study, intranasal delivery of Mn to C57BL/6 mice induced significant deficits in motor behavior. Our Mn treatment paradigm also depleted TH in the olfactory bulb (OB) region of the brain and increased expression of the astrocyte activation marker GFAP. In contrast, Dorman *et al.* (2004) did not observe upregulation of GFAP in the rat OB after 90 days of Mn exposure. This discrepancy may be attributed to species differences (mice vs. rats) and application of different Mn compounds ($MnCl_2$ vs. $MnSO_4$). Our studies also reveal that Mn increased the levels of pro-inflammatory cytokines (Fig. 8). Mn is known to accumulate in the striatum, but with this acute treatment paradigm, we did not observe any changes in striatal dopamine or GFAP. Longer chronic studies are required to determine the relationship between dopamine and GFAP levels in the striatum of Mn-treated mice. Our study collectively demonstrates that Mn can 1) induce mitochondrial damage by altering mitochondrial dynamics and bioenergetic states in astrocytes, 2) increase production of proinflammatory factors in astrocytes, 3) potentiate αSyn_{agg}-induced inflammation in astrocytes, further validating the gene-environment relationship, and 4) induce astrocyte activation and TH loss in the OB, leading to OB inflammation and decreased motor activity when administered intranasally *in vivo*. Our novel findings provide an important insight into how the environmental toxicant Mn modulates inflammation and metabolic activity in astrocytes. Future studies should explore the variable mechanistic basis of astrocyte-mediated neuroinflammation in Mn neurotoxicity.

Acknowledgments

This work was supported by National Institutes of Health (NIH) Grants: ES026892 and NS088206. The authors would like to thank Dr. Balaraman Kalyanaraman for providing access to Mito-apocynin. Lloyds chair to AGK and Salsbury Chair to AK are also acknowledged.

References

Alfonso-Loeches S, Urena-Peralta JR, Morillo-Bargues MJ, Oliver-De La Cruz J, Guerri C. Role of mitochondria ROS generation in ethanol-induced NLRP3 inflammasome activation and cell death in astroglial cells. Front Cell Neurosci. 2014; 8:216. [PubMed: 25136295]

Alvarez-Erviti L, Couch Y, Richardson J, Cooper JM, Wood MJ. Alpha-synuclein release by neurons activates the inflammatory response in a microglial cell line. Neurosci Res. 2011; 69(4):337–342. [PubMed: 21255620]

Amor S, Puentes F, Baker D, van der Valk P. Inflammation in neurodegenerative diseases. Immunology. 2010; 129(2):154–169. [PubMed: 20561356]

Aschner M, Gannon M, Kimelberg HK. Manganese uptake and efflux in cultured rat astrocytes. J Neurochem. 1992; 58(2):730–735. [PubMed: 1729413]

Bichell TJ, Wegrzynowicz M, Grace Tipps K, Bradley EM, Uhouse MA, Bryan M, Horning K, Fisher N, Dudek K, Halbesma T, Umashanker P, Stubbs AD, Holt HK, Kwakye GF, Tidball AM, Colbran RJ, Aschner M, Diana Neely M, Di Pardo A, Maglione V, Osmand A, Bowman AB. Reduced bioavailable manganese causes striatal urea cycle pathology in Huntington's disease mouse model. Biochim Biophys Acta. 2017

Bihaqi SW, Zawia NH. Enhanced taupathy and AD-like pathology in aged primate brains decades after infantile exposure to lead (Pb). Neurotoxicology. 2013; 39:95–101. [PubMed: 23973560]

Blecharz-Klin K, Piechal A, Joniec-Maciejak I, Pyrzanowska J, Widy-Tyszkiewicz E. Effect of intranasal manganese administration on neurotransmission and spatial learning in rats. Toxicol Appl Pharmacol. 2012; 265(1):1–9. [PubMed: 23022103]

Brenza TM, Ghaisas S, Ramirez JE, Harischandra D, Anantharam V, Kalyanaraman B, Kanthasamy AG, Narasimhan B. Neuronal protection against oxidative insult by polyanhydride nanoparticle-based mitochondria-targeted antioxidant therapy. Nanomedicine. 2016

Charli A, Jin H, Anantharam V, Kanthasamy A, Kanthasamy AG. Alterations in mitochondrial dynamics induced by tebufenpyrad and pyridaben in a dopaminergic neuronal cell culture model. Neurotoxicology. 2016; 53:302–313. [PubMed: 26141520]

Chen CJ, Liao SL. Oxidative stress involves in astrocytic alterations induced by manganese. Exp Neurol. 2002; 175(1):216–225. [PubMed: 12009774]

Chen P, Bowman AB, Mukhopadhyay S, Aschner M. SLC30A10: A novel manganese transporter. Worm. 2015; 4(3):e1042648. [PubMed: 26430566]

Choi CJ, Anantharam V, Martin DP, Nicholson EM, Richt JA, Kanthasamy A, Kanthasamy AG. Manganese upregulates cellular prion protein and contributes to altered stabilization and proteolysis: relevance to role of metals in pathogenesis of prion disease. Toxicol Sci. 2010; 115(2): 535–546. [PubMed: 20176619]

Choi CJ, Anantharam V, Saetveit NJ, Houk RS, Kanthasamy A, Kanthasamy AG. Normal cellular prion protein protects against manganese-induced oxidative stress and apoptotic cell death. Toxicol Sci. 2007; 98(2):495–509. [PubMed: 17483122]

Codolo G, Plotegher N, Pozzobon T, Brucale M, Tessari I, Bubacco L, de Bernard M. Triggering of inflammasome by aggregated alpha-synuclein, an inflammatory response in synucleinopathies. PLoS One. 2013; 8(1):e55375. [PubMed: 23383169]

Colombo E, Farina C. Astrocytes: Key Regulators of Neuroinflammation. Trends Immunol. 2016; 37(9):608–620. [PubMed: 27443914]

Dorman DC, McManus BE, Marshall MW, James RA, Struve MF. Old age and gender influence the pharmacokinetics of inhaled manganese sulfate and manganese phosphate in rats. Toxicol Appl Pharmacol. 2004; 197(2):113–124. [PubMed: 15163547]

Ellingsen DG, Hetland SM, Thomassen Y. Manganese air exposure assessment and biological monitoring in the manganese alloy production industry. J Environ Monit. 2003; 5(1):84–90. [PubMed: 12619760]

Febbraro F, Giorgi M, Caldarola S, Loreni F, Romero-Ramos M. alpha-Synuclein expression is modulated at the translational level by iron. Neuroreport. 2012; 23(9):576–580. [PubMed: 22581044]

Freeman LC, Ting JP. The pathogenic role of the inflammasome in neurodegenerative diseases. J Neurochem. 2016; 136(1):29–38. [PubMed: 26119245]

Galvin JE, Giasson B, Hurtig HI, Lee VM, Trojanowski JQ. Neurodegeneration with brain iron accumulation, type 1 is characterized by alpha-, beta-, and gamma-synuclein neuropathology. Am J Pathol. 2000; 157(2):361–368. [PubMed: 10934140]

Gavin CE, Gunter KK, Gunter TE. Manganese and calcium efflux kinetics in brain mitochondria Relevance to manganese toxicity. Biochem J. 1990; 266(2):329–334. [PubMed: 2317189]

Ghosh A, Langley MR, Harischandra DS, Neal ML, Jin H, Anantharam V, Joseph J, Brenza T, Narasimhan B, Kanthasamy A, Kalyanaraman B, Kanthasamy AG. Mitoapocynin Treatment Protects Against Neuroinflammation and Dopaminergic Neurodegeneration in a Preclinical Animal Model of Parkinson's Disease. J Neuroimmune Pharmacol. 2016a; 11(2):259–278. [PubMed: 26838361]

Ghosh A, Saminathan H, Kanthasamy A, Anantharam V, Jin H, Sondarva G, Harischandra DS, Qian Z, Rana A, Kanthasamy AG. The peptidyl-prolyl isomerase Pin1 up-regulation and proapoptotic function in dopaminergic neurons: relevance to the pathogenesis of Parkinson disease. J Biol Chem. 2013; 288(30):21955–21971. [PubMed: 23754278]

Ghosh A, Tyson T, George S, Hildebrandt EN, Steiner JA, Madaj Z, Schulz E, Machiela E, McDonald WG, Escobar Galvis ML, Kordower JH, Van Raamsdonk JM, Colca JR, Brundin P. Mitochondrial

pyruvate carrier regulates autophagy, inflammation, and neurodegeneration in experimental models of Parkinson's disease. Sci Transl Med. 2016b; 8(368):368ra174.

Giasson BI, Uryu K, Trojanowski JQ, Lee VM. Mutant and wild type human alpha-synucleins assemble into elongated filaments with distinct morphologies in vitro. J Biol Chem. 1999; 274(12):7619–7622. [PubMed: 10075647]

Glass CK, Saijo K, Winner B, Marchetto MC, Gage FH. Mechanisms underlying inflammation in neurodegeneration. Cell. 2010; 140(6):918–934. [PubMed: 20303880]

Golde TE. Inflammation takes on Alzheimer disease. Nat Med. 2002; 8(9):936–938. [PubMed: 12205453]

Gonzalez LE, Juknat AA, Venosa AJ, Verrengia N, Kotler ML. Manganese activates the mitochondrial apoptotic pathway in rat astrocytes by modulating the expression of proteins of the Bcl-2 family. Neurochem Int. 2008; 53(6-8):408–415. [PubMed: 18930091]

Gordon R, Hogan CE, Neal ML, Anantharam V, Kanthasamy AG, Kanthasamy A. A simple magnetic separation method for high-yield isolation of pure primary microglia. J Neurosci Methods. 2011; 194(2):287–296. [PubMed: 21074565]

Gordon R, Neal ML, Luo J, Langley MR, Harischandra DS, Panicker N, Charli A, Jin H, Anantharam V, Woodruff TM, Zhou QY, Kanthasamy AG, Kanthasamy A. Prokineticin-2 upregulation during neuronal injury mediates a compensatory protective response against dopaminergic neuronal degeneration. Nature communications. 2016; 7:12932.

Gordon R, Neal ML, Luo J, Langley MR, Harischandra DS, Panicker N, Charli A, Jin H, Anantharam V, Woodruff TM, Zhou QY, Kanthasamy AG, Kanthasamy A. Prokineticin-2 upregulation during neuronal injury mediates a compensatory protective response against dopaminergic neuronal degeneration. Nature communications. 2016a; 7:12932.

Gordon R, Singh N, Lawana V, Ghosh A, Harischandra DS, Jin H, Hogan C, Sarkar S, Rokad D, Panicker N, Anantharam V, Kanthasamy AG, Kanthasamy A. Protein kinase Cdelta upregulation in microglia drives neuroinflammatory responses and dopaminergic neurodegeneration in experimental models of Parkinson's disease. Neurobiology of disease. 2016b; 93:96–114. [PubMed: 27151770]

Gorojod RM, Alaimo A, Porte Alcon S, Pomilio C, Saravia F, Kotler ML. The autophagic- lysosomal pathway determines the fate of glial cells under manganese-induced oxidative stress conditions. Free radical biology & medicine. 2015; 87:237–251. [PubMed: 26163003]

Graff CL, Pollack GM. Nasal drug administration: potential for targeted central nervous system delivery. J Pharm Sci. 2005; 94(6):1187–1195. [PubMed: 15858850]

Gregory A, Polster BJ, Hayflick SJ. Clinical and genetic delineation of neurodegeneration with brain iron accumulation. J Med Genet. 2009; 46(2):73–80. [PubMed: 18981035]

Gunter RE, Puskin JS, Russell PR. Quantitative magnetic resonance studies of manganese uptake by mitochondria. Biophys J. 1975; 15(4):319–333. [PubMed: 236048]

Gunter TE, Gavin CE, Aschner M, Gunter KK. Speciation of manganese in cells and mitochondria: a search for the proximal cause of manganese neurotoxicity. Neurotoxicology. 2006; 27(5):765–776. [PubMed: 16765446]

Gunter TE, Sheu SS. Characteristics and possible functions of mitochondrial Ca(2+) transport mechanisms. Biochim Biophys Acta. 2009; 1787(11):1291–1308. [PubMed: 19161975]

Harischandra DS, Ghaisas S, Rokad D, Zamanian M, Jin H, Anantharam V, Kimber M, Kanthasamy A, Kanthasamy A. Environmental Neurotoxicant Manganese Regulates Exosome-mediated Extracellular miRNAs in Cell Culture Model of Parkinson's Disease: Relevance to alpha-Synuclein Misfolding in Metal Neurotoxicity. Neurotoxicology. 2017

Harischandra DS, Jin H, Anantharam V, Kanthasamy A, Kanthasamy AG. alpha-Synuclein protects against manganese neurotoxic insult during the early stages of exposure in a dopaminergic cell model of Parkinson's disease. Toxicol Sci. 2015; 143(2):454–468. [PubMed: 25416158]

Hazell AS. Astrocytes and manganese neurotoxicity. Neurochem Int. 2002; 41(4):271–277. [PubMed: 12106778]

Herrero MT, Estrada C, Maatouk L, Vyas S. Inflammation in Parkinson's disease: role of glucocorticoids. Front Neuroanat. 2015; 9:32. [PubMed: 25883554]

Hesketh S, Sassoon J, Knight R, Brown DR. Elevated manganese levels in blood and CNS in human prion disease. Mol Cell Neurosci. 2008; 37(3):590–598. [PubMed: 18234506]

Horning KJ, Caito SW, Tipps KG, Bowman AB, Aschner M. Manganese Is Essential for Neuronal Health. Annu Rev Nutr. 2015; 35:71–108. [PubMed: 25974698]

Kanthasamy AG, Choi C, Jin H, Harischandra DS, Anantharam V, Kanthasamy A. Effect of divalent metals on the neuronal proteasomal system, prion protein ubiquitination and aggregation. Toxicol Lett. 2012; 214(3):288–295. [PubMed: 22995398]

Karki P, Lee E, Aschner M. Manganese neurotoxicity: a focus on glutamate transporters. Ann Occup Environ Med. 2013; 25(1):4. [PubMed: 24472696]

Karki P, Smith K, Johnson J Jr, Aschner M, Lee E. Role of transcription factor yin yang 1 in manganese-induced reduction of astrocytic glutamate transporters: Putative mechanism for manganese-induced neurotoxicity. Neurochem Int. 2015; 88:53–59. [PubMed: 25128239]

Karki P, Webb A, Smith K, Johnson J Jr, Lee K, Son DS, Aschner M, Lee E. Yin Yang 1 is a repressor of glutamate transporter EAAT2, and it mediates manganese-induced decrease of EAAT2 expression in astrocytes. Mol Cell Biol. 2014; 34(7):1280–1289. [PubMed: 24469401]

Kim C, Ho DH, Suk JE, You S, Michael S, Kang J, Joong Lee S, Masliah E, Hwang D, Lee HJ, Lee SJ. Neuron-released oligomeric alpha-synuclein is an endogenous agonist of TLR2 for paracrine activation of microglia. Nature communications. 2013; 4:1562.

Kwakye GF, Paoliello MM, Mukhopadhyay S, Bowman AB, Aschner M. Manganese-Induced Parkinsonism and Parkinson's Disease: Shared and Distinguishable Features. Int J Environ Res Public Health. 2015; 12(7):7519–7540. [PubMed: 26154659]

Langley M, Ghosh A, Charli A, Sarkar S, Ay M, Luo J, Zielonka J, Brenza T, Bennett B, Jin H, Ghaisas S, Schlichtmann B, Kim D, Anantharam V, Kanthasamy A, Narasimhan B, Kalyanaraman B, Kanthasamy A. Mito-apocynin Prevents Mitochondrial Dysfunction, Microglial Activation, Oxidative Damage and Progressive Neurodegeneration in MitoPark Transgenic Mice. Antioxidants & Redox Signaling. 2017

Lawana V, Singh N, Sarkar S, Charli A, Jin H, Anantharam V, Kanthasamy AG, Kanthasamy A. Involvement of c-Abl Kinase in Microglial Activation of NLRP3 Inflammasome and Impairment in Autolysosomal System. J Neuroimmune Pharmacol. 2017

Lee EJ, Woo MS, Moon PG, Baek MC, Choi IY, Kim WK, Junn E, Kim HS. Alpha-synuclein activates microglia by inducing the expressions of matrix metalloproteinases and the subsequent activation of protease-activated receptor-1. Journal of immunology. 2010; 185(1):615–623.

Leyva-Illades D, Chen P, Zogzas CE, Hutchens S, Mercado JM, Swaim CD, Morrisett RA, Bowman AB, Aschner M, Mukhopadhyay S. SLC30A10 is a cell surface-localized manganese efflux transporter, and parkinsonism-causing mutations block its intracellular trafficking and efflux activity. The Journal of neuroscience : the official journal of the Society for Neuroscience. 2014; 34(42):14079–14095. [PubMed: 25319704]

Liu L, Chan C. IPAF inflammasome is involved in interleukin-1beta production from astrocytes, induced by palmitate; implications for Alzheimer's Disease. Neurobiology of aging. 2014; 35(2): 309–321. [PubMed: 24054992]

Liu T, Xue CC, Shi YL, Bai XJ, Li ZF, Yi CL. Overexpression of mitofusin 2 inhibits reactive astrogliosis proliferation in vitro. Neurosci Lett. 2014; 579:24–29. [PubMed: 25017825]

Lotharius J, Brundin P. Pathogenesis of Parkinson's disease: dopamine, vesicles and alpha-synuclein. Nat Rev Neurosci. 2002; 3(12):932–942. [PubMed: 12461550]

Luk KC, Kehm V, Carroll J, Zhang B, O'Brien P, Trojanowski JQ, Lee VM. Pathological alpha-synuclein transmission initiates Parkinson-like neurodegeneration in nontransgenic mice. Science. 2012a; 338(6109):949–953. [PubMed: 23161999]

Luk KC, Kehm VM, Zhang B, O'Brien P, Trojanowski JQ, Lee VM. Intracerebral inoculation of pathological alpha-synuclein initiates a rapidly progressive neurodegenerative alpha-synucleinopathy in mice. J Exp Med. 2012b; 209(5):975–986. [PubMed: 22508839]

Malthankar GV, White BK, Bhushan A, Daniels CK, Rodnick KJ, Lai JC. Differential lowering by manganese treatment of activities of glycolytic and tricarboxylic acid (TCA) cycle enzymes investigated in neuroblastoma and astrocytoma cells is associated with manganese-induced cell death. Neurochem Res. 2004; 29(4):709–717. [PubMed: 15098932]

Martinez-Finley EJ, Gavin CE, Aschner M, Gunter TE. Manganese neurotoxicity and the role of reactive oxygen species. Free radical biology & medicine. 2013; 62:65–75. [PubMed: 23395780]

Milatovic D, Yin Z, Gupta RC, Sidoryk M, Albrecht J, Aschner JL, Aschner M. Manganese induces oxidative impairment in cultured rat astrocytes. Toxicol Sci. 2007; 98(1):198–205. [PubMed: 17468184]

Mittal M, Siddiqui MR, Tran K, Reddy SP, Malik AB. Reactive oxygen species in inflammation and tissue injury. Antioxid Redox Signal. 2014; 20(7):1126–1167. [PubMed: 23991888]

Moberly AH, Czarnecki LA, Pottackal J, Rubinstein T, Turkel DJ, Kass MD, McGann JP. Intranasal exposure to manganese disrupts neurotransmitter release from glutamatergic synapses in the central nervous system in vivo. Neurotoxicology. 2012; 33(5):996–1004. [PubMed: 22542936]

Moreno JA, Streifel KM, Sullivan KA, Legare ME, Tjalkens RB. Developmental exposure to manganese increases adult susceptibility to inflammatory activation of glia and neuronal protein nitration. Toxicol Sci. 2009; 112(2):405–415. [PubMed: 19812365]

Moreno JA, Sullivan KA, Carbone DL, Hanneman WH, Tjalkens RB. Manganese potentiates nuclear factor-kappaB-dependent expression of nitric oxide synthase 2 in astrocytes by activating soluble guanylate cyclase and extracellular responsive kinase signaling pathways. J Neurosci Res. 2008; 86(9):2028–2038. [PubMed: 18335517]

Narhi L, Wood SJ, Steavenson S, Jiang Y, Wu GM, Anafi D, Kaufman SA, Martin F, Sitney K, Denis P, Louis JC, Wypych J, Biere AL, Citron M. Both familial Parkinson's disease mutations accelerate alpha-synuclein aggregation. J Biol Chem. 1999; 274(14):9843–9846. [PubMed: 10092675]

Ngwa HA, Kanthasamy A, Jin H, Anantharam V, Kanthasamy AG. Vanadium exposure induces olfactory dysfunction in an animal model of metal neurotoxicity. Neurotoxicology. 2014; 43:73–81. [PubMed: 24362016]

Panicker N, Saminathan H, Jin H, Neal M, Harischandra DS, Gordon R, Kanthasamy K, Lawana V, Sarkar S, Luo J, Anantharam V, Kanthasamy AG, Kanthasamy A. Fyn Kinase Regulates Microglial Neuroinflammatory Responses in Cell Culture and Animal Models of Parkinson's Disease. The Journal of neuroscience : the official journal of the Society for Neuroscience. 2015; 35(27):10058–10077. [PubMed: 26157004]

Park EJ, Park K. Induction of oxidative stress and inflammatory cytokines by manganese chloride in cultured T98G cells, human brain glioblastoma cell line. Toxicol In Vitro. 2010; 24(2):472–479. [PubMed: 19815061]

Pekny M, Pekna M. Astrocyte reactivity and reactive astrogliosis: costs and benefits. Physiol Rev. 2014; 94(4):1077–1098. [PubMed: 25287860]

Peres TV, Schettinger MR, Chen P, Carvalho F, Avila DS, Bowman AB, Aschner M. Manganese-induced neurotoxicity: a review of its behavioral consequences and neuroprotective strategies. BMC Pharmacol Toxicol. 2016; 17(1):57. [PubMed: 27814772]

Pham AH, Meng S, Chu QN, Chan DC. Loss of Mfn2 results in progressive, retrograde degeneration of dopaminergic neurons in the nigrostriatal circuit. Hum Mol Genet. 2012; 21(22):4817–4826. [PubMed: 22859504]

Phillips EC, Croft CL, Kurbatskaya K, O'Neill MJ, Hutton ML, Hanger DP, Garwood CJ, Noble W. Astrocytes and neuroinflammation in Alzheimer's disease. Biochem Soc Trans. 2014; 42(5):1321–1325. [PubMed: 25233410]

Popoli M, Yan Z, McEwen BS, Sanacora G. The stressed synapse: the impact of stress and glucocorticoids on glutamate transmission. Nat Rev Neurosci. 2011; 13(1):22–37. [PubMed: 22127301]

Rao KV, Norenberg MD. Manganese induces the mitochondrial permeability transition in cultured astrocytes. J Biol Chem. 2004; 279(31):32333–32338. [PubMed: 15173181]

Rodier J. Manganese poisoning in Moroccan miners. Br J Ind Med. 1955; 12(1):21–35. [PubMed: 14351643]

Rokad D, Ghaisas S, Harischandra DS, Jin H, Anantharam V, Kanthasamy A, Kanthasamy AG. Role of neurotoxicants and traumatic brain injury in alpha-synuclein protein misfolding and aggregation. Brain Res Bull. 2016

Sarkar S, Malovic E, Plante B, Zenitsky G, Jin H, Anantharam V, Kanthasamy A, Kanthasamy AG. Rapid and Refined CD11b Magnetic Isolation of Primary Microglia with Enhanced Purity and Versatility. J Vis Exp. 2017; (122)

Scott I, Youle RJ. Mitochondrial fission and fusion. Essays in biochemistry. 2010; 47:85–98. [PubMed: 20533902]

Seo J, Ottesen EW, Singh RN. Antisense methods to modulate pre-mRNA splicing. Methods Mol Biol. 2014; 1126:271–283. [PubMed: 24549671]

Sidoryk-Wegrzynowicz M, Aschner M. Role of astrocytes in manganese mediated neurotoxicity. BMC Pharmacol Toxicol. 2013; 14:23. [PubMed: 23594835]

Streifel KM, Miller J, Mouneimne R, Tjalkens RB. Manganese inhibits ATP-induced calcium entry through the transient receptor potential channel TRPC3 in astrocytes. Neurotoxicology. 2013; 34:160–166. [PubMed: 23131343]

Su X, Maguire-Zeiss KA, Giuliano R, Prifti L, Venkatesh K, Federoff HJ. Synuclein activates microglia in a model of Parkinson's disease. Neurobiology of aging. 2008; 29(11):1690–1701. [PubMed: 17537546]

Tang FL, Liu W, Hu JX, Erion JR, Ye J, Mei L, Xiong WC. VPS35 Deficiency or Mutation Causes Dopaminergic Neuronal Loss by Impairing Mitochondrial Fusion and Function. Cell Rep. 2015; 12(10):1631–1643. [PubMed: 26321632]

Tansey MG, Goldberg MS. Neuroinflammation in Parkinson's disease: its role in neuronal death and implications for therapeutic intervention. Neurobiology of disease. 2010; 37(3):510–518. [PubMed: 19913097]

Tjalkens RB, Zoran MJ, Mohl B, Barhoumi R. Manganese suppresses ATP-dependent intercellular calcium waves in astrocyte networks through alteration of mitochondrial and endoplasmic reticulum calcium dynamics. Brain Res. 2006; 1113(1):210–219. [PubMed: 16934782]

Volterra A, Meldolesi J. Astrocytes, from brain glue to communication elements: the revolution continues. Nat Rev Neurosci. 2005; 6(8):626–640. [PubMed: 16025096]

Whitton PS. Inflammation as a causative factor in the aetiology of Parkinson's disease. Br J Pharmacol. 2007; 150(8):963–976. [PubMed: 17339843]

Yen CF, Harischandra DS, Kanthasamy A, Sivasankar S. Copper-induced structural conversion templates prion protein oligomerization and neurotoxicity. Sci Adv. 2016; 2(7):e1600014. [PubMed: 27419232]

Yin Z, Aschner JL, dos Santos AP, Aschner M. Mitochondrial-dependent manganese neurotoxicity in rat primary astrocyte cultures. Brain Res. 2008; 1203:1–11. [PubMed: 18313649]

Highlights

1. Mn induces mitochondrial dysfunction in astrocytes
2. Mn exposure induces inflammatory response in astrocytes and exacerbates αSyn_{agg}-induced inflammatory response in astrocytes
3. Mito-apocynin attenuates Mn-induced inflammatory response in astrocytes by reducing mitochondrial damage
4. Intranasal Mn exposure induces neuroinflammation and behavioral deficits in mouse model
5. Thus, Mn-induced mitochondrial defects contributes to astroglial neuroinflammation

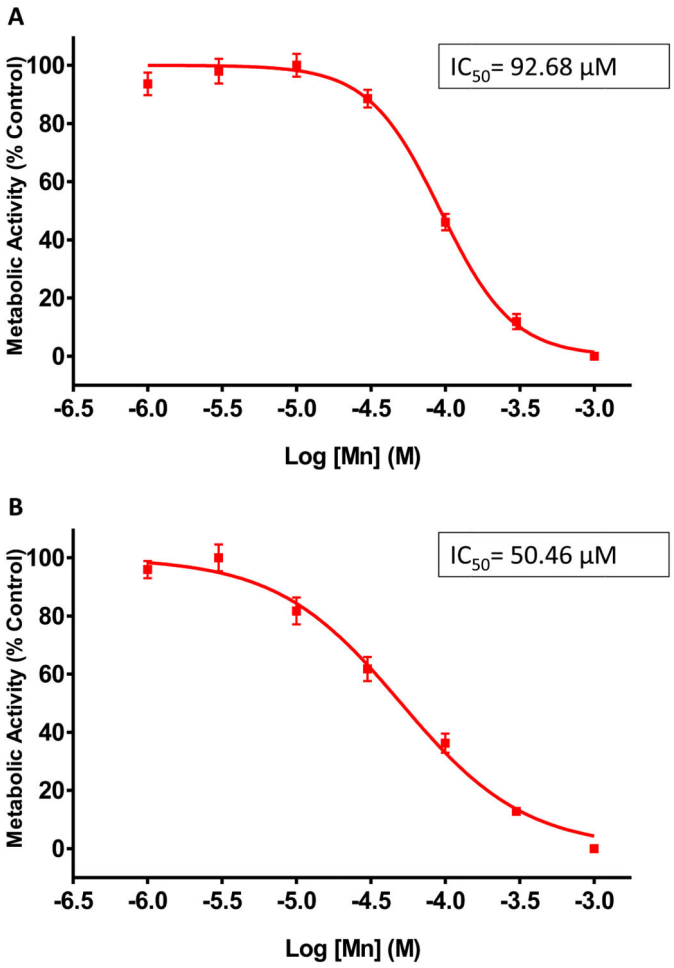

Fig. 1. Determination of IC_{50} for $MnCl_2$ based on metabolic response of astrocytic cell culture

(A) MTS assay performed on primary mouse astrocytes after treatment with 1, 3, 10, 30, 100, 300, and 1000 µM $MnCl_2$ for 24 h. (B) MTS assay performed on U373 human astrocyte cell line after treatment with 1, 3, 10, 30, 100, 300, and 1000 µM $MnCl_2$ for 24 h. Data represented as mean±SEM with 8 biological replicates from 1-2 independent experiments.

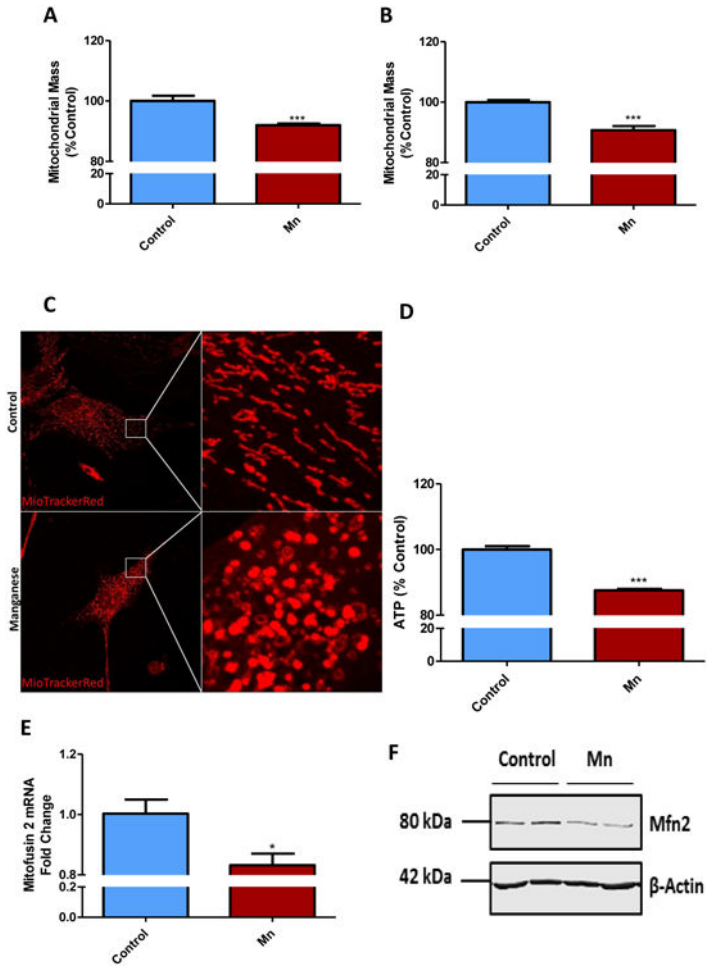

Fig. 2. Mn exposure reduced mitochondrial mass and induced mitochondrial dysfunction in astrocyte cell cultures

100 μM Mn for 24 h induced loss in mitochondrial mass in primary mouse astrocytes (A) and in U373 cell line (B), as shown by MitoTracker green assay. (C) 100 μM Mn exposure shifted mitochondrial morphology in primary astrocytes, as shown by MitoTracker Red. (D) CellTiter Glo assay reveals Mn reduced ATP production in primary astrocytes. (E) q-RT-PCR and (F) Western blot analyses show 100 μM Mn exposure for 24 h reduced Mitofusin2 (Mfn2) in primary mouse astrocytes. Data analyzed via Student's t test, *p<0.05, **p<0.01, ***p<0.001. Data represented as mean±SEM with 3-8 biological replicates from 2-3 independent experiments.

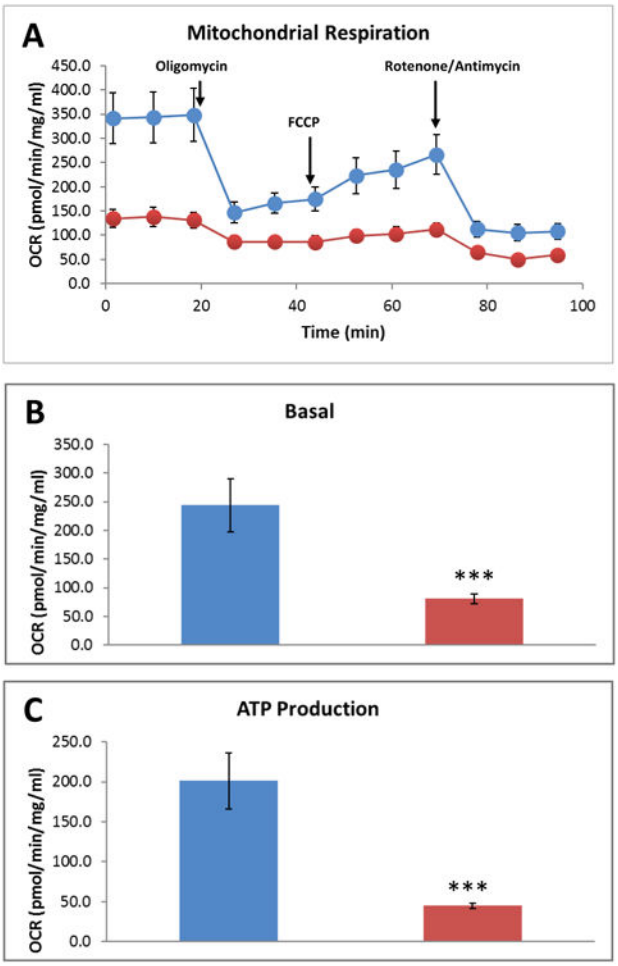

Fig. 3. Mn exposure altered mitochondrial respiration in primary mouse astrocytes

(A) Seahorse Mito Stress Test measuring oxygen consumption rate (OCR). Mn exposure for 24 h reduced basal mitochondrial respiration (B) and mitochondrial ATP generation (C) in primary mouse astrocytes. Data analyzed via Student's t test, *p<0.05, **p <0.01, ***p<0.001. Data represented as mean±SEM with 3-5 biological replicates from 2-3 independent experiments.

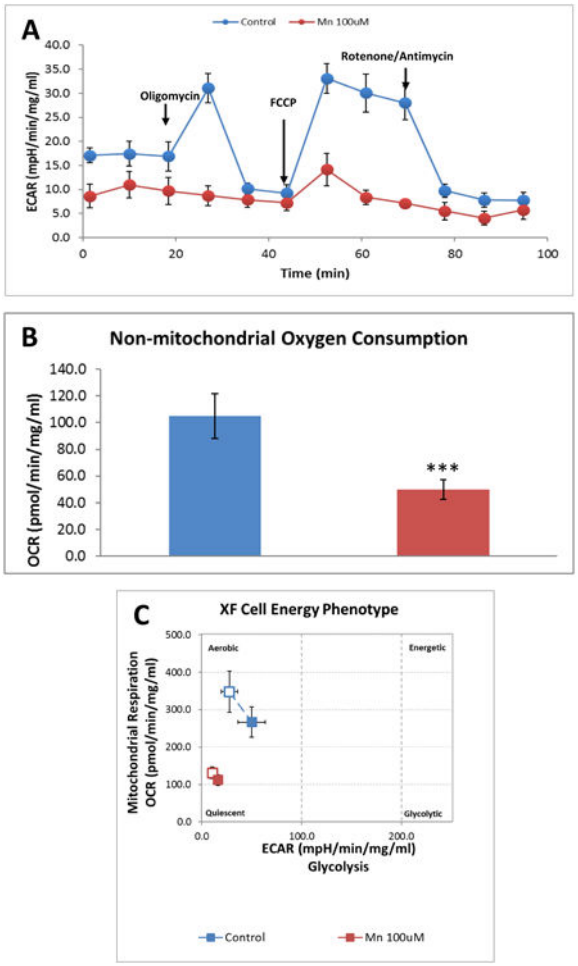

Fig. 4. Mn exposure alters non-mitochondrial respiration and cellular energy phenotype in primary mouse astrocytes

(A) Seahorse Mito-Stress Test measuring extracellular acidification rate (ECAR). Mn exposure for 24 h reduced non-mitochondrial respiration (B). 100 μM Mn altered cellular energy phenotype in primary mouse astrocytes (C). Data analyzed via Student's t-test, *p<0.05, **p <0.01, ***p<0.001. Data represented as mean±SEM with 3-5 biological replicates from 2-3 independent experiments.

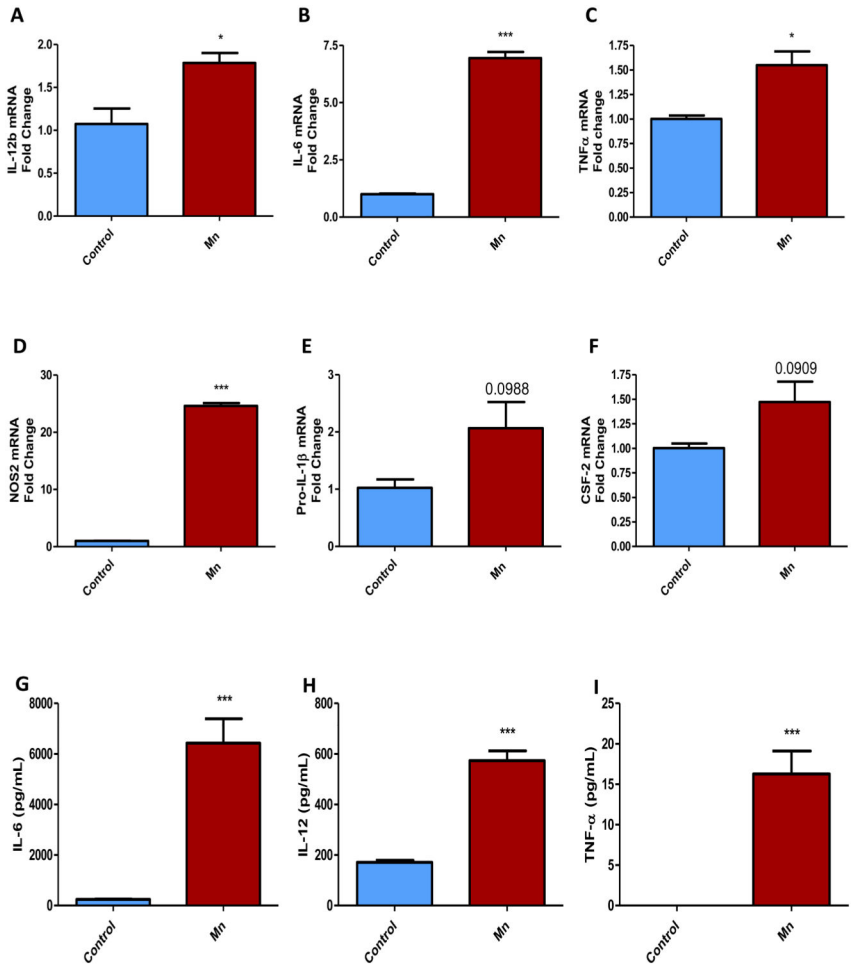

Fig. 5. Mn-induced production of pro-inflammatory factors in astrocytes

(A-F) q-RT-PCR analysis of primary mouse astrocytes treated with 100 μM Mn for 24 h induced expression of the pro-inflammatory factors IL-12b (A), IL-6 (B), TNFα (C), Nos2 (D), pro-IL-1β (E) and GM-CSF (F). (G-I) Luminex analysis of treatment medium from primary astrocytes exposed to 100 μM Mn for 24 h, revealing induction of the released pro-inflammatory factors IL-6 (G), IL-12 (H), TNFα (I). Data analyzed via Student's t-test, *p<0.05, **p <0.01, ***p<0.001. Data represented as mean±SEM with 2-8 biological replicates from 2-3 independent experiments.

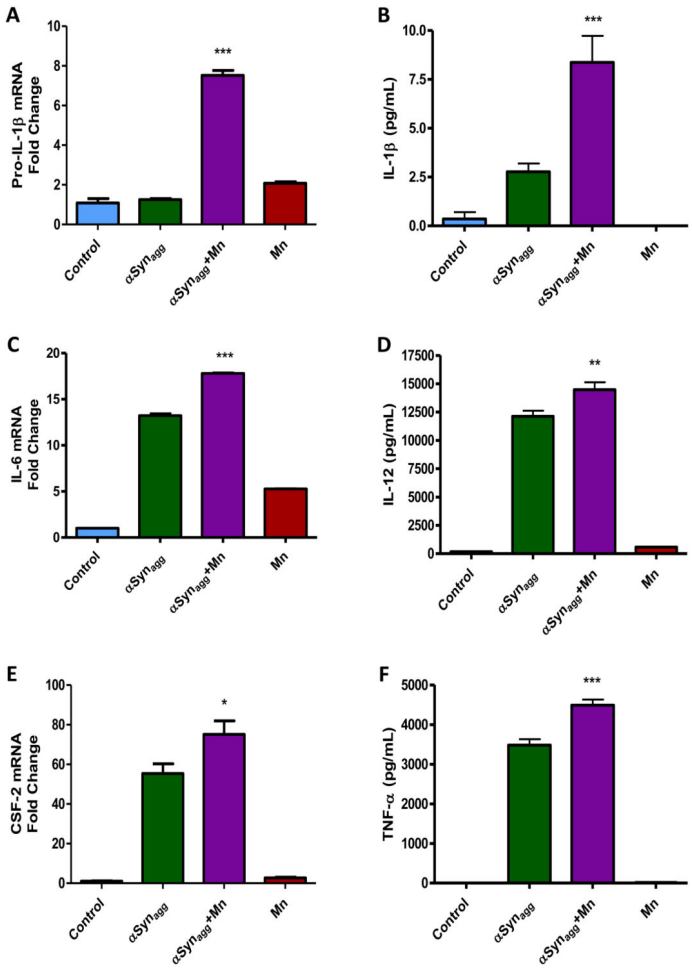

Fig. 6. Mn potentiated production and release of pro-inflammatory factors induced by αSyn$_{agg}$

(A) Co-treatment of 100 μM Mn with 1 μM αSyn$_{agg}$ (Agg-αsyn) potentiated pro-IL-1β mRNA levels as shown by q-RT-PCR. (B) Luminex assay reveals Mn potentiated release of IL-1β levels from astrocytes induced by αSyn$_{agg}$. (C, E) Mn aggravated αSyn$_{agg}$-induced mRNA expression of IL-6 (C) and GM-CSF (E) as revealed by q-RT-PCR. (D, F) Luminex assay showing Mn has an additive effect on the release of αSyn$_{agg}$-induced IL-12 (D) and TNFα (F). Data analyzed via ANOVA with Tukey post analysis, *p<0.05, **p <0.01, ***p<0.001. Data represented as mean±SEM with 3-8 biological replicates from 2-3 independent experiments.

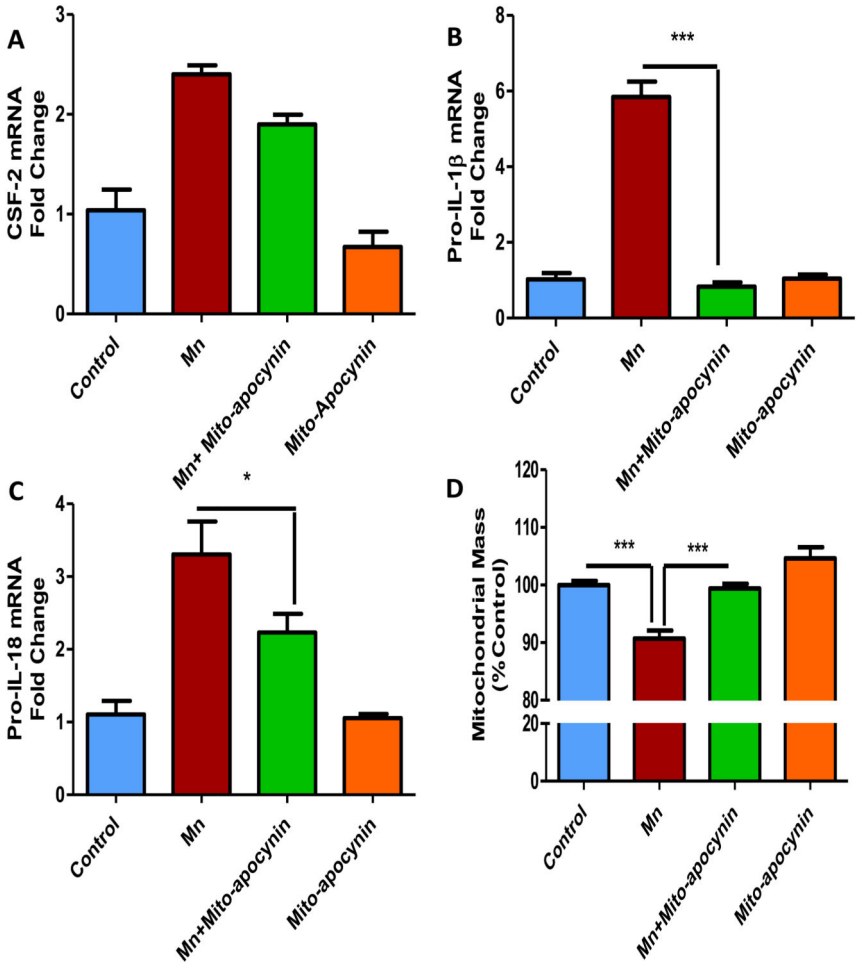

Fig. 7. Mito-apocynin attenuated Mn-induced pro-inflammatory factors in human astrocytic culture

Co-treatment with 10 μM mito-apocynin (MA) and 100 μM $MnCl_2$ attenuated the mRNA upregulation of GM-CSF (A), pro-IL-1β (B) and pro-IL-18 (C). (D) Co-treatment with 10 μM mito-apocynin and 100 μM $MnCl_2$ modulated the change in mitochondrial mass induced by Mn, as shown by MitoTracker Green assay. Data analyzed via ANOVA with Tukey post analysis, *p<0.05, **p<0.01, ***p<0.001. Data represented as mean±SEM with 3-8 biological replicates from 2-3 independent experiments.

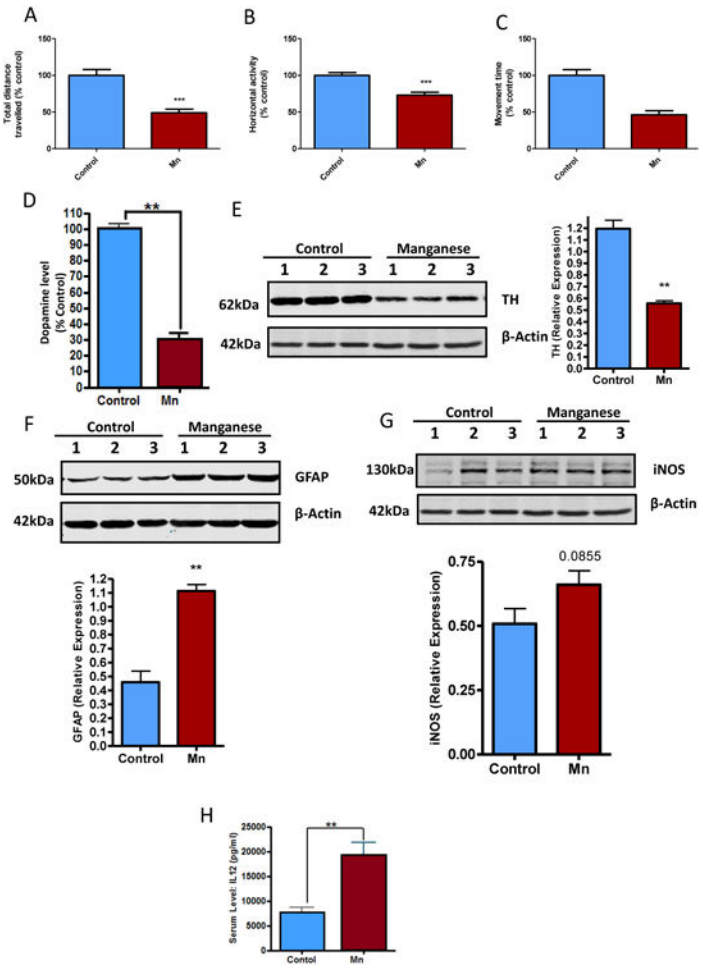

Fig. 8. Intranasal exposure to Mn caused motor deficits and inflammation *in vivo*

(A-C) Intranasal exposure of 50 μl of 20 mM $MnCl_2$ caused motor deficits in C57BL/6 mice as indicated by total distance traveled (A), horizontal activity, (B) and total movement time (C). Neurochemical analysis of OB revealing Mn reduced dopamine levels (D). Western blot analysis shows Mn reduced TH (E) and increased GFAP (F) and iNOS (G). (H) Luminex analysis shows Mn exposure increased serum levels of IL-12. Data analyzed via Student's t-test, *p<0.05, **p<0.01, ***p<0.001. Data represented as mean±SEM with n=6-16.